

# Shedding Light on Luminescence Lifetime Measurement and Associated Data Treatment

Waygen Thor, Jean-Claude G. Bünzli,\* Ka-Leung Wong,\* and Peter A. Tanner\*

Luminescence lifetime is a crucial parameter in photophysical studies that bears essential physical and chemical information and that is used to quantify a variety of phenomena, from the determination of quenching mechanisms to temperature sensing and bioimaging. The current perception of lifetime measurement is that it is a trivial and fast experiment. However, despite this apparent simplicity, measuring luminescence decay and fitting the obtained data to a suitable model can be far more intricate. In this perspective, the influence of experimental parameters and fitting procedures on the determination of lifetimes are investigated and, through carefully chosen examples, it is shown that large variations, up to 10%, can be induced by varying parameters such as the data acquisition time, the baseline evaluation, or the mathematical fitting model. In order to present to a wider audience, detailed mathematical descriptions are kept out of the manuscript.

## 1. Introduction

After being populated, a specific luminescent species releases photons over time with a first-order steady-state kinetics decay characterized by a rate constant  $k$  [s<sup>-1</sup>].

$$I(t) = I(0)\exp^{-kt} \quad (1a)$$

The associated luminescence lifetime  $\tau$  [s] is an important experimentally determined parameter which is defined as  $1/k$  or as the time after the excitation pulse for the light intensity to drop to  $1/e$  ( $\approx 1/2.71828\dots$ ) of the initial value  $I(0)$ .<sup>[1]</sup> Taking natural logarithms of Equation (1a) we have:

$$\ln I(t) = \ln I(0) - kt \quad (1b)$$

The lifetime reflects not only radiative processes, but all the deactivation routes of the luminescent state. We can classify these in short as emission of photons (described by the radiative lifetime,  $\tau_r$ ) and all other nonradiative routes (which we simplify as the nonradiative lifetime,  $\tau_{nr}$ ), according to:

$$\frac{1}{\tau} = \frac{1}{\tau_r} + \frac{1}{\tau_{nr}} = k_r + \sum k_{nr} = k \quad (2)$$


Emission lifetimes can vary over 15–16 orders of magnitude; for example, they are in the ps–ns range for singlet emission of organic materials ( $S_1 \rightarrow S_0$ ), ns range for electric dipole (ED) allowed transitions of

di- or tri-positive lanthanide ions ( $4f^{n-1}5d \rightarrow 4f^n$ ),  $\mu$ s–s range for spin-forbidden triplet emission of aromatic compounds ( $T_1 \rightarrow S_0$ ),  $\mu$ s range for magnetic dipole (MD) allowed transitions of transition metals or lanthanides,  $\mu$ s–ms range for forced ED  $4f^n \rightarrow 4f^n$  transitions of lanthanides, and to second-hour regimes for persistent luminescence (Figure 1).

The measured lifetime can be used to: 1) indicate the purity of a sample, since it should be strictly monoexponential for a pure analyte if no processes occur other than light emission and nonradiative decay from the luminescent level; 2) reveal and characterize the different luminescent species when emission spectra overlap;<sup>[2]</sup> 3) distinguish static and dynamic quenching mechanisms of luminescence; 4) estimate the energy transfer efficiency,  $\eta_{ET}$ , from a donor to an acceptor:  $\eta_{ET} = 1 - \frac{\tau}{\tau_0}$  where  $\tau$  and  $\tau_0$  are the lifetimes of the donor in the presence and absence of the acceptor, respectively; 5) measure temperature, for example, *in cellulo*<sup>[3]</sup> or *in vivo*;<sup>[4]</sup> 6) perform luminescence lifetime bioimaging,<sup>[5]</sup> particularly of deep tissues;<sup>[6]</sup> 7) determine activation energies of quenching mechanisms.<sup>[7]</sup> Detailed reviews are available for the techniques and implementation of lifetime measurements,<sup>[8]</sup> and we attempt not to overlap with these. Rather, we focus on the time-domain determination of lifetimes and analysis methodology, and by carefully selected examples, we present experimental evidence that measurement conditions and data treatment procedures may considerably influence the final estimated value of the lifetime. We limit our quest to compounds with decay lifetime in the time span from ns to s, but present data for solid state samples and solutions, inorganic or organic. For each sample, focus is made on a particular aspect of the experimental procedure and/or of the sample characteristics. The chemical structures, syntheses of

W. Thor, J.-C. G. Bünzli, K.-L. Wong, P. A. Tanner  
Department of Applied Biology and Chemical Technology  
The Hong Kong Polytechnic University  
Kowloon, Hong Kong S.A.R.  
E-mail: jean-claude.bunzli@epfl.ch; klgwong@polyu.edu.hk;  
peter.a.tanner@gmail.com

J.-C. G. Bünzli  
Institute of Chemical Sciences and Engineering  
Swiss Federal Institute of Technology, Lausanne (EPFL)  
1015 Lausanne, Switzerland

 The ORCID identification number(s) for the author(s) of this article can be found under <https://doi.org/10.1002/adpr.202400081>.

© 2024 The Author(s). Advanced Photonics Research published by Wiley-VCH GmbH. This is an open access article under the terms of the Creative Commons Attribution License, which permits use, distribution and reproduction in any medium, provided the original work is properly cited.

DOI: 10.1002/adpr.202400081

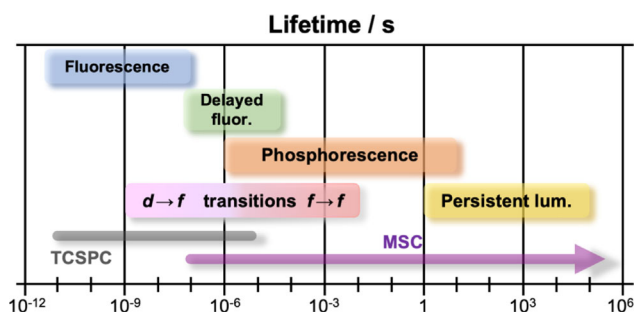


**Figure 1.** Approximate time ranges for common luminescence processes. The grey and violet bars below point to the time-domains ideal for the two main experimental techniques used to determine lifetimes, TCSPC (time-correlated single-photon counting) and MSC (multichannel scaling); fluor. fluorescence, lum. luminescence.

samples and instrumentation employed are described in the Supporting Information.

## 2. Examples of Fitting Luminescence Decay Curves

There are two main experimental techniques for measuring luminescence decays. The first one simply measures luminescence intensity at a given emission wavelength following the excitation pulse (typically 10 Hz repetition rate) and in a constant time window that is swept over the entire measurement time. The output is a graph of photon counts versus time and the method is sometimes referred to as multi-channel scaling (MSC).<sup>[9]</sup> In the second technique (TCSPC) the sample is excited by a high-repetition light source (typically 1 MHz) and one single photon is detected after each pulse, and a histogram of photon arrival times on the detector, measured with ps precision, is established;<sup>[10a]</sup> a variant of this technique is the analog mean delay (AMD) method that can detect multiple photons simultaneously.<sup>[10b]</sup> The common time domain for which these two techniques are used is shown in Figure 1.

Although seemingly simple, the determination of lifetimes is prone to several experimental problems/artefacts. Common ones are 1) detector saturation by too large signals so that the linear relationship between the number of photons emitted and the signal intensity is lost; 2) excessively noisy emission in the case of weak emitters; 3) non-constant baseline; or 4) spurious signal due to interference from the excitation lamp pulse that is extremely intense so that it is not always totally removed by filters/monochromators – not to mention photodecomposition of the sample or an insufficiently cleaned sample cuvette/holder! We stress here the absolute need to proceed to a blank measurement before starting lifetime determination on the sample. In addition, we show below that the model used to fit the data and the sampling time domain of the data set also play non-negligible roles.

An additional point is error reporting. When fitting a luminescence decay with a given model, standard deviation calculations are provided, often summarized with the adjusted coefficient of determination  $R^2_{\text{adj}}$  (1 meaning a perfect fit), and with standard

deviations affecting each parameter, particularly the lifetime. These deviations are usually very small when the model is correct. One must keep in mind that they are intimately linked to the model used, are of a statistical nature, and do not correspond to the experimental error that should be reported. The latter should consider reproducibility of the experiment, if possible, by measuring each sample at least thrice, measuring 2–3 samples of the investigated material, and, also, checking the influence of the measurement parameters (data recording parameters), and of the chosen data treatment model. If this is not possible, at least replicate samples should be obtained and measured. Since the subject of this work is the influence of data treatment, most of the lifetimes reported here have exceedingly small (or zero) associated fitting uncertainties.

### 2.1. Testing a Monoexponential Decay: Which Formula to Use? Is It Really Monoexponential?

In the following, the decays have been measured by a photomultiplier and displayed 1) as the number of photons emitted at a given wavelength at time  $t$ ,  $I(t)$ ; or 2) through an oscilloscope, in voltage -  $\mu\text{V}$  or  $\text{mV}$ . Normalization is often performed on data to focus on the underlying distribution shape. This is either made by setting the most intense value of  $I(t)$  to 1; or in  $[0,1]$  normalization, by setting the smallest one to 0 and the most intense value of  $I(t)$  to 1. The same value of lifetime results from a monoexponential decay fit of the original data or for either of these two alternatives, but other parameters may vary. For a logarithmic ordinate, normalization is essential if some data are negative.

The equations most often used to fit a dataset exhibiting monoexponential decay are:

$$I(t) = I_b + I(0)\exp(-t/\tau) \quad (3a)$$

where, compared with Equation (1a), the baseline correction,  $I_b$ , is inserted in software such as Origin or others. If this is not a freely varying parameter, the baseline counts can be taken as the value before the light pulse, if possible, otherwise as the value approached at, or after, the end time of the data recording.

Alternatively, a linear fit of the form  $y = a + bt$  is made by taking logarithms:

$$\log_{10}(I(t) - I_b) = \log_{10}I(0) - 0.43429t/\tau \quad (3b(i))$$

Or natural logarithms:

$$\ln(I(t) - I_b) = \ln I(0) - t/\tau \quad (3b(ii))$$

In these equations  $t$  [s] is time and  $\tau$  [s] is the lifetime. At time  $t = 0$ , for a dataset  $[0,1]$  normalized, we expect that  $I(0) + I_b = 1$ , but this will not be the case for a fit where there is an incorrect baseline or deviation from monoexponentiality. Normally, the optional Equation (3a(ii)), rather than Equation (3b(ii)), is chosen because the ordinate is clearer in powers of ten. The linear fit then has the slope  $-0.43429.../\tau$ . The minimizing problems of an exponential fit (Equation (3a)) and a logarithm-linear fit (Equation (3b)) are different (as described in the Supporting Information for an Eu(III) helicate, Section 2.1.1, Figure S1, Table S1, Supporting Information) so that one should also be prepared to obtain a different result if both equations are

employed. Besides, taking logarithms compresses the data and minimizes the sum of squares error (SSE) for the transformed data, whereas the exponential fits minimize the SSE for the original data.

The Guggenheim (Equation (3c)) and Phase-Plane methods are available for fitting exponential data with constant, but unknown baselines.<sup>[11]</sup> In the linear fit of the Guggenheim method,  $y = \ln[I(t) - I(t + \Delta t)]$  (note that it usually employs  $\ln$  rather than  $\log$ ) is plotted against time,  $t$ , in an equation of the form  $y = a + bt$ :

$$\ln[I(t) - I(t + \Delta t)] = \ln\{K[1 - \exp(-\Delta t/\tau)]\} - t/\tau \quad (3c)$$

where  $\Delta t$  represents the increment between readings and should be in the region at least  $2\tau$  to  $3\tau$ ;  $K$  is a fitting constant. The linear slope  $b$  is  $-1/\tau$ . The Guggenheim method is popular because it eliminates the need for acquiring a base line, gives accurate measurements, and is simple.

**Figure 2a** shows the room-temperature (RT) emission spectrum of  $[\text{Yb}(\text{TTA})_3\text{phen}]$  (TTA = thenoyltrifluoroacetate,

phen = 1,10-phenanthroline). The sample has not been recrystallized and excitation was performed through the ligand level at 355 nm, taking advantage of the antenna effect. The emission occurs from the  $^2F_{5/2}$  to the  $^2F_{7/2}$  J-multiplet. The data fits according to Equation (3a) and (3b(i)), and (3c) for the timescale 0–195  $\mu\text{s}$  are displayed in Figure 2b–d and Figure S2 and S3 (Supporting Information) and the results are listed in **Table 1**. The table not only shows the comparison between the fits using the different equations, but also the effect of constraining some parameters and reducing the number of freely varying ones.

There is a significant difference between the 3-parameter monoexponential fit (Item 1) and the 2- (Items 3–5) or 1- (Item 2) parameter linear fits in this case! Moreover, one sees the great importance of the baseline choice since the difference in resulting parameters between the constrained choices of  $I_b = 0$  (Item 3) and  $I_b = 4.0404\text{E-}3$  (Item 4) (i.e., choosing the value fitted in Figure 2b, Item 1) is enormous. The  $I(0)$  values also differ considerably for Items 1,3 and 4. The Guggenheim method yields a result 13.5% different from the exponential fit.

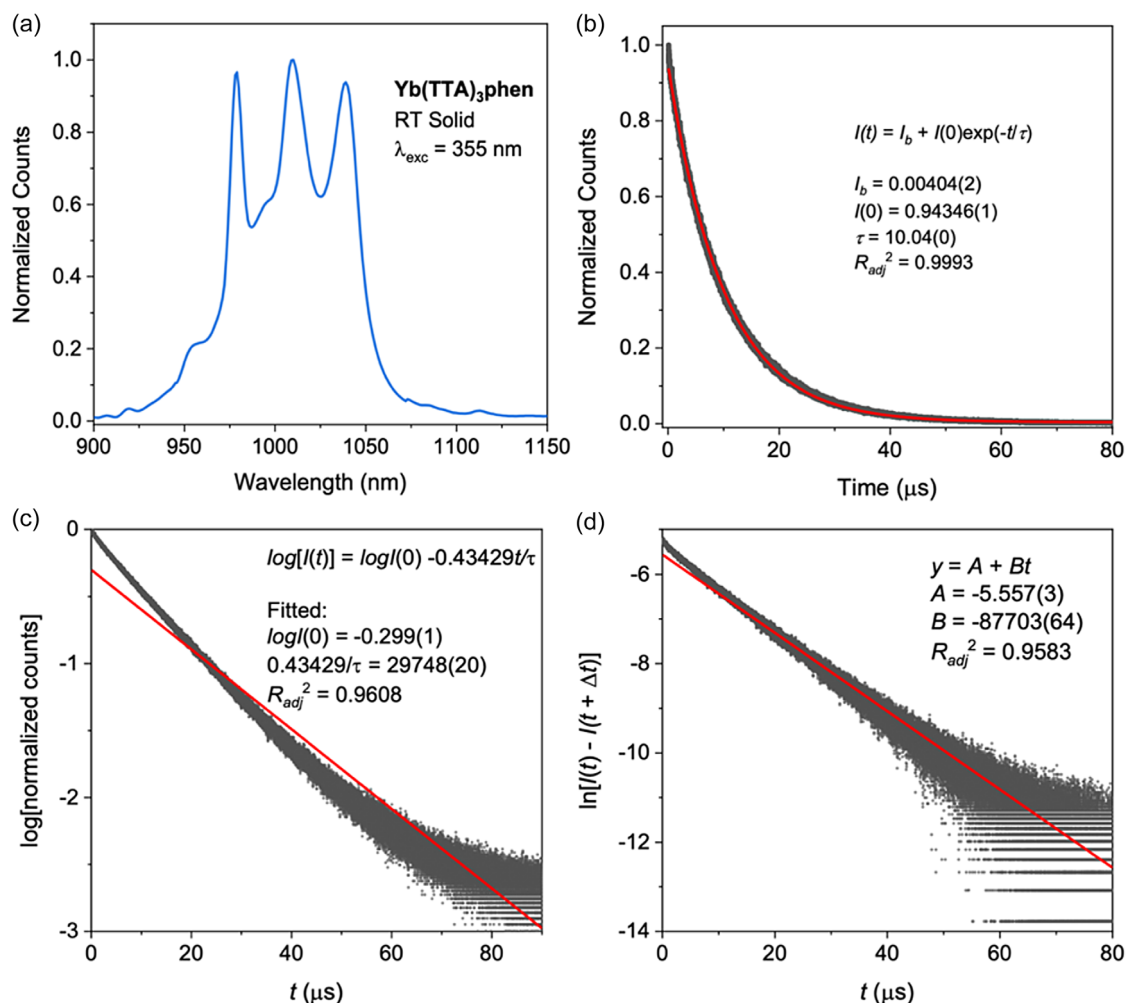


**Figure 2.** a) 355 nm excited room temperature emission spectrum of  $[\text{Yb}(\text{TTA})_3\text{phen}]$  in the solid state. b,c) Luminescence decay measured at 995 nm. The data have been normalized [0,1] in Origin. b) The fit with Equation (3a) and c) using Equation (3b(i)). d) Guggenheim fit of the same data with  $\Delta t = 20 \mu\text{s}$ . Refer to Table 1 for fitted lifetimes.

**Table 1.** Comparison of exponential and linear fits of the monoexponential decay of an un-recrystallized solid-state sample of [Yb(TTA)<sub>3</sub>phen] in the range 0–195 μs. Excitation wavelength: 355 nm, analyzing wavelength: 995 nm; 94 744 time data.

Item	Equation	Figure	N <sup>a)</sup>	I <sup>b)</sup>	I(0)	τ [μs]	R <sup>2</sup> <sub>adj</sub>
1	(3a)	2b	3	4.04(2)E-3	0.94346(1)	10.04(0)	0.9993
2	(3bi)	S2	1	[0]	[1]	12.59(0)	0.9864
3	(3bi)	2c	2	[0]	0.502(1)	14.60(0)	0.9608
4	(3bi)	S3	2	[4.04E-3]	1.158(5)	9.25(0)	0.9676
5	(3c)	2d	2	n.a.	n.a.	11.40(1)	0.9583

<sup>a)</sup>N is the number of freely varying parameters. <sup>b)</sup>Here, and in the following, the bracketed number represents the standard deviation as applied to the last significant figure(s). R<sup>2</sup><sub>adj</sub> is the adjusted coefficient of determination of the fit. The square brackets represent that the parameter is constrained in the fit; n.a. not applicable. The value of Δt in the Guggenheim fit was fixed near 2τ (i.e., at 20 μs). Refer to the Supporting Information for the discussion of items 2–4.

However, visual examination of the two linear fits Equation (3b) and (3c) is extremely useful since it enables one to assess the deviation from exponentiality, as represented here by the deviation from linearity. This deviation occurs because there is an initial fast decay. Hence, to answer the question in the title of this section, one can see from this deviation that the data do not well represent monoexponential decay. Fitting the dataset with a double exponential function (Figure S4, Supporting Information) yields lifetimes of 3.08 and 10.67 μs, with the longer lifetime weighted 8.8 times more than the short lifetime. The fitted longer lifetime differs from that of the monoexponential fit by 6%.

In fact, this example is a perfect illustration of the use of lifetime measurements to assess the purity of a sample. The compound [Yb(TTA)<sub>3</sub>phen] has previously been reported to exhibit monoexponential decay with the lifetime of 12.01 ± 0.02 μs in the solid state,<sup>[12]</sup> 10.4 and 11.9 μs in toluene and CCl<sub>4</sub>,<sup>[13]</sup> respectively. The present sample preparation was not conducted in an inert atmosphere and the compound was not recrystallized. The deviation from monoexponential decay for our sample indicates sample impurity.

### 2.1.1. Conclusions

The type of fit, choice of baseline, and number of freely varying parameters all considerably influence the value of the fitted lifetime. When data have been normalized [0,1], the fitted parameter I(0) should be close to 1.0, and I<sub>b</sub> should be zero, which is not the case in the examples above. These fitted values, in addition to the observation of nonlinearity in the logarithmic plot, indicate deviations from monoexponentiality.

The largest deviations of the parameter R<sup>2</sup><sub>adj</sub> occur for the linear fit methods and the smallest for the fit with Equation (3a). In addition to a monoexponential fit, it is good to employ a linear representation to visually investigate deviations from monoexponential decay. Otherwise, a high value of R<sup>2</sup><sub>adj</sub> ≈ 1 in the former fit (as in Figure 2b) might encourage one to think that the dataset

clearly represents monoexponential decay and that the sample is pure. The present exercise puts in perspective the reporting of lifetimes with 2–3 significant digits in the literature.

## 2.2. Fitting a Biexponential Rise and Decay Function Curve

We consider here the case where both the population (k<sub>D</sub>) and depopulation (k<sub>A</sub>) kinetics of the excited state have been measured. This type of experiment offers insight into the mechanism of the excited state population but often necessitates sophisticated equipment because the population kinetics can be extremely fast. There are exceptions though, particularly when it comes to the luminescence of lanthanide ions.

Figure 3a shows the room temperature <sup>5</sup>D<sub>0</sub> emission spectrum of Y<sub>2</sub>O<sub>3</sub>:Eu<sup>3+</sup>. The luminescence decay after a short laser pulse is displayed in Figure 3b. The intensity rise occurs due to nonradiative energy transfer from the higher-lying donor state to <sup>5</sup>D<sub>0</sub>, with subsequent nonradiative and radiative decays from the <sup>5</sup>D<sub>0</sub> level to the <sup>7</sup>F<sub>J</sub> manifold (J = 0–6) (Figure 3c). The considered donor state to <sup>5</sup>D<sub>0</sub> is <sup>5</sup>D<sub>1</sub>. The overall kinetics of <sup>5</sup>D<sub>0</sub> emission is not first-order, so an appropriate fit is required. The graph can be fitted (in red) by the donor–acceptor biexponential function:

$$I(t) = A \exp^{-\frac{t}{\tau_A}} - B \exp^{-\frac{t}{\tau_D}} + I_b \quad (4)$$

where A and B are constants; I<sub>b</sub>, usually a parameter in the fitting equation, represents the baseline counts; and τ<sub>A</sub> and τ<sub>D</sub> are the lifetimes of the emissive (acceptor, <sup>5</sup>D<sub>0</sub>) and populating (donor, <sup>5</sup>D<sub>1</sub>) states, respectively, shown in Figure 3c. The time to maximum emission intensity is denoted by t<sub>max</sub>, where for pulsed excitation:<sup>[14]</sup>

$$t_{\max} = \left\{ \frac{1}{[\tau_D^{-1} - \tau_A^{-1}]} \right\} \ln \left[ \frac{\tau_A}{\tau_D} \right] \quad (5)$$

and the total time monitored is denoted by t<sub>total</sub>. Here, we have measured t<sub>max</sub> from the experimental rise and decay graph of <sup>5</sup>D<sub>0</sub>, with the dataset normalized [0,1], as in Figure 3b. The fit to Equation (4) in Figure 3b, where (t<sub>total</sub>/t<sub>max</sub> = 38.5) gives reliable parameter values, as shown in the figure: τ<sub>D</sub> = τ<sub>D1</sub> = 96.6 μs, τ<sub>A</sub> = τ<sub>D0</sub> = 1.17 ms, and t<sub>max</sub> = 0.26 ms.

However, fitting the decay over short time spans, t<sub>total</sub>/t<sub>max</sub> < 4 gives unrealistic values of τ<sub>A</sub> and τ<sub>D</sub>. Then, when t<sub>total</sub>/t<sub>max</sub> increases beyond ≈3.7, there is a big change in parameter values, and the values gradually become closer to those of Figure 3b, as shown in Figure 3d. Both lifetime values are only slightly dependent upon the iteration algorithm employed (the Levenberg Marquardt here, but we also used Orthogonal Distance Regression). Moreover, the parameter I<sub>b</sub> has been freely varied in these fits and displays the same abrupt change around the ratio t<sub>total</sub>/t<sub>max</sub> ≈ 3.7 (Figure S6, Supporting Information).

Subtraction of the baseline in Figure 3b, so that the constant values near 10 ms correspond to zero counts, gives the same lifetime parameters as in Figure 3b, using Equation (4). However, if the value of the parameter I<sub>b</sub> is constrained in the fitting, using an inaccurate value can lead to large errors in the lifetimes τ<sub>A</sub> and τ<sub>D</sub>. Figure 3d displays values of these lifetimes, together

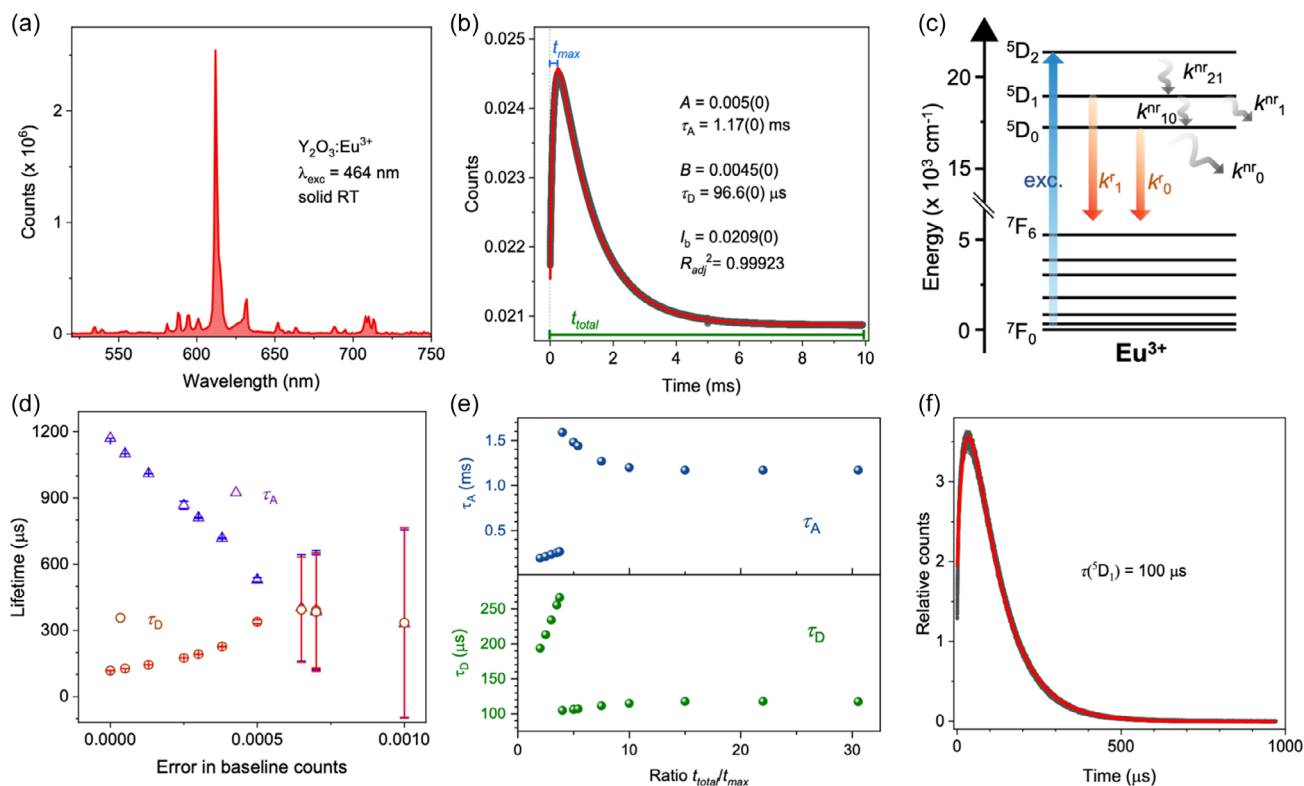


**Figure 3.** a) 464 nm ( $^5D_2$ ) excited room temperature emission spectrum of  $Y_2O_3$  doped with 1 at.%  $Eu^{3+}$ . b) Emission rise and decay measured at 611 nm under 464 nm excitation. The monitoring time,  $t_{total}$ , is shown to extend to the end of the data set in this case. The fit, in red, uses Equation (4). c) Schematic diagram of relevant energy levels and decay processes. The full upward vertical arrow represents population of  $^5D_2$ , followed by nonradiative decay to  $^5D_1$ . Wavy downward arrows represent nonradiative processes, whilst straight ones represent radiative ones. The lifetime of  $^5D_1$ ,  $\tau_{D_1}$ , is given by:  $\frac{1}{\tau_{D_1}} = k_1^r + k_1^{nr} + k_{10}^{nr}$ ; and the lifetime of  $^5D_0$ ,  $\tau_{D_0}$ , is given by  $\frac{1}{\tau_{D_0}} = k_0^r + k_0^{nr}$ , where the  $k$  are rate constants. d) Values and errors of the fitted lifetimes  $\tau_A$  and  $\tau_D$  when inaccurate values are fixed for the baseline. Refer to Figure S7 and Table S1 (Supporting Information). e) Variation of fitted acceptor,  $\tau_A$ , and donor,  $\tau_D$ , lifetimes according to Equation (4), with increasing monitoring time,  $t_{total}$ , relative to time to maximum intensity,  $t_{max}$ . The error bars in the fits lie inside the points. The acceptor A is  $^5D_0$  and the donor D is  $^5D_1$ . f) Rise and decay of  $^5D_1$  luminescence. The fitted  $^5D_1$  lifetime using Equation (4) is given as 100  $\mu s$  and the rise time for  $^5D_2 \rightarrow ^5D_1$  is 25  $\mu s$ .

with the fitting errors, for various fixed errors in baseline counts (Figure S7, Table S2, Supporting Information).

The point of this rather involved discussion is to emphasize that the total time taken for data fitting can have a severe impact upon the calculated lifetime values. The decay timespan  $t_{total}$  needs to be appropriate, i.e., long enough so that the function can appropriately fit the decay part of the curve. Moreover, it seems better to keep the baseline  $I_b$  as an adjustable parameter.

In this example, the rise time of  $^5D_0$  (Figure 3b) is equal to the decay lifetime of  $^5D_1$ , the kinetics of which is displayed in Figure 3f, in line with the assumed energy transfer mechanism (Figure 3c).

### 2.2.1. Conclusion

When fitting biexponential rise and decay functions, make sure that the decay tail is long. The monitoring time,  $t_{total}$ , needs to be  $\approx 10$  times that of  $t_{max}$  in the present case to reach correct lifetimes. Hence, it is advised to check the values of the lifetimes when using different monitoring times. Equation (5) is useful for checking the value of  $t_{max}$  after the two lifetimes have been

fitted and then estimating if the considered  $t_{total}$  value is long enough.

### 2.3. For What Range Should We Measure Lifetime?

Literature data often report monoexponential lifetimes without stating the measurement (i.e., the fitting) range. However, the lifetime value would change if another timescale range were employed. We demonstrate this with a dinuclear europium helicate  $[Eu_2(L^{C2})_3]$  at 15  $\mu M$  concentration in 0.1 M tris buffer (pH 7.4), excited at 355 nm into the ligand levels.<sup>[15]</sup> The fit of the entire decay (0–12.5 ms) with Equation (3a) in Figure 4a is reasonably good ( $R_{adj}^2 = 0.9989$ ), except at the beginning, and yields the reported literature value  $\tau = 2.43$  ms.<sup>[14]</sup> Trimming the first 0.30 ms results in a slightly better fit ( $R_{adj}^2 = 0.9990$ ) with a shorter lifetime, 2.37 ms (Figure S8a, Supporting Information). Trimming more data points at the beginning of the decay leads to a smooth decrease of the lifetime from 2.43 to 2.22 ms when the first 2 ms of data are removed. This tendency is the same if the fit is stopped at 11 ms instead of 12.5 ms (Figure S8b, Supporting Information).



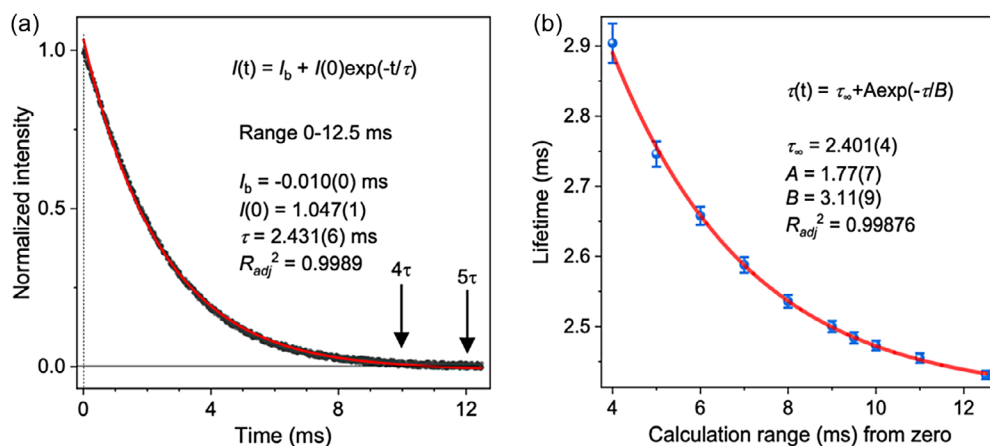


**Figure 4.** a) Room temperature  $^5D_0$  emission decay of a europium helicate  $[Eu_2(L^{C2})_3]$  at 15  $\mu M$  concentration in tris buffer.<sup>[15]</sup> b) Plot of fitted monoexponential lifetime values when employing shorter calculation ranges ( $t$  ms) than starting at 0 ms up to 12.5 ms.

Shortening the fitting time of the decay curve is revealed to have a more important effect on the lifetime value. Figure 4b indicates a continuous increase of the calculated lifetime from 2.43 ms to 2.90 ms when the fitting range is shortened from 12.5 to 4 ms. This figure can be fitted with a monoexponential function as indicated and the fitted value of  $\tau$  at infinite time ( $\tau_\infty$ ) is 2.40 ms. The decay curve only approaches zero in Figure 4a after  $\approx 11$  ms so recording the decay for at least five lifetimes appears to be compelling, with longer measurement times being recommended.

To summarize the behavior of the fitted lifetime in the present example: it decreases with increasing measurement time (Figure 4b), while decreasing when the initial portion trimmed at the beginning is longer (Figure S8, Supporting Information). We do not offer explanations for these observations, but we perceive that the variations are of importance. For instance, if the fit is stopped at  $3\tau$  or if it starts at  $0.5\tau$ , variations in the present case with respect to the fit in Figure 4a amount to 6.6% and 3.3%, respectively. A further example, with varying data measurement times in the ns range, is given later in Figure 7e,f.

### 2.3.1. Conclusions

Fit the lifetime decay curve over a range of  $>5$  lifetimes (10 being recommended). The  $R_{adj}^2$  parameter measures the proportion of the variance in the dependent variable (normalized intensity) that is predictable from the independent variable (time) in the regression model, adjusted for the number of parameters employed. The highest value of this parameter at a certain calculation range may not correspond to the “true” value of the lifetime because the range may not be optimal.

### 2.4. For What Wavelength Should We Measure Lifetime Decay? the Case of YAG:Ce<sup>3+</sup>

Figure 5a displays the RT emission spectrum of yttrium aluminum garnet ( $Y_3Al_5O_{12}$ , YAG) doped with 0.5 and 5 at.% Ce<sup>3+</sup> while the decay curves are illustrated in Figure S10

(Supporting Information). For the higher concentration of Ce<sup>3+</sup>, the excitation spectrum is broader because Ce<sup>3+</sup> occupies more diverse sites and Ce<sup>3+</sup>-Ce<sup>3+</sup> interaction is stronger, whereas the emission spectrum is red-shifted due to self-absorption.<sup>[16]</sup> The relevant energy levels of Ce<sup>3+</sup> are shown in Figure 5b. It has been shown that for different Ce<sup>3+</sup> systems, the reciprocal lifetime is proportional to the electric dipole moment matrix element squared, the wavelength to the power  $-3$ , and a Lorentz refractive index term.<sup>[17]</sup> Other studies have shown that for different fluorescent proteins, the fluorescence lifetime decreases as the emission wavelength increases.<sup>[18]</sup> We investigate herein the results for one system, YAG:Ce<sup>3+</sup>, with emission from one excited state,  $5d_1$ . We anticipated that the Ce<sup>3+</sup> lifetime would be independent of the wavelength monitored,<sup>[19]</sup> but other studies have concluded that the lifetime varies as  $\lambda^{-2}$ .<sup>[20]</sup> For one excited state in a fixed environment, the lifetime comprises all radiative and nonradiative processes and is constant with measured wavelength. If not, other factors are at play, such as emission from ions in slightly different environments.

With excitation at 460 nm into the intense absorption band, since the emission spectrum is broad, what wavelength should we use to monitor the lifetime? Despite the fact that most studies monitor the lifetime at the emission maximum, it is worth noting that the saturation of the detector should be considered to prevent an instrumental artifact. If the wavelength chosen is overlapping with the region for self-absorption, the lifetime measured can be affected and is normally lengthened.<sup>[21]</sup>

The decay curves are not exact monoexponential functions and have been fitted with both Equation (3a) and the biexponential Equation (6), where both parameters  $A$  and  $B$  are positive:

$$I(t) = A\exp^{-t/\tau_1} + B\exp^{-t/\tau_2} + I_b \quad (6)$$

Experimental results for the emission decay of the YAG:Ce<sup>3+</sup> sample at different wavelengths are fitted in Figure 5c on a log scale and the resulting lifetimes from monoexponential and biexponential fits are plotted in Figure 5d. Shorter lifetimes are usually associated with Ce<sup>3+</sup> ions near defects, at surface sites, or

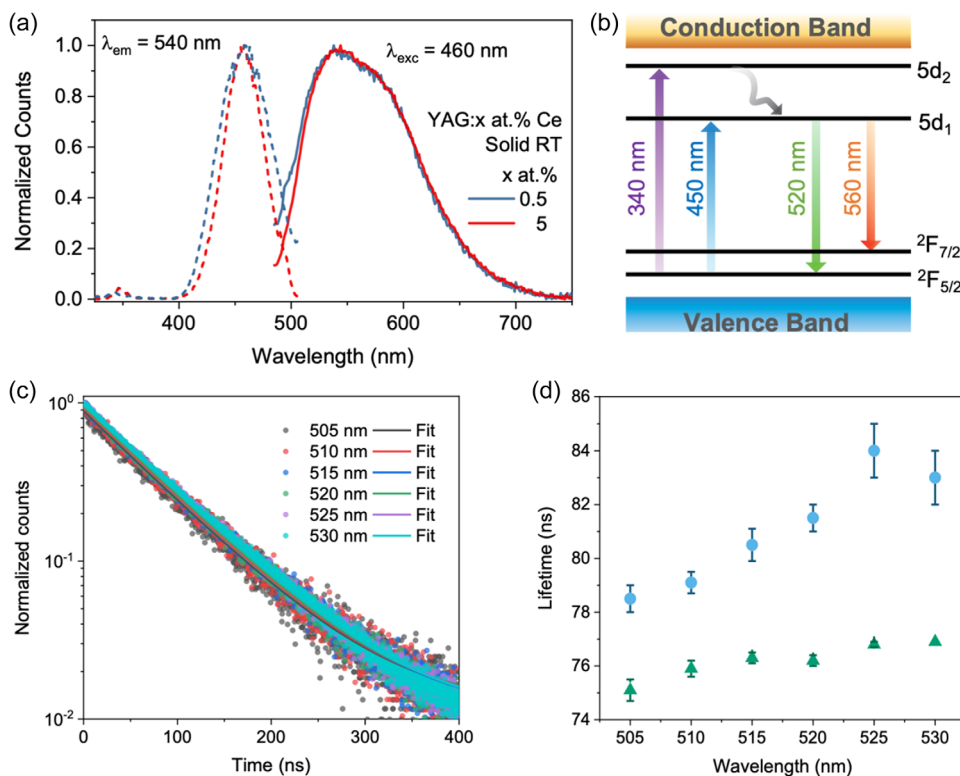


**Figure 5.** a) 460 nm excited RT emission and 540 nm excitation spectra of YAG doped with 5 and 0.5 at.%  $Ce^{3+}$ . b) Scheme of relevant energy levels: 5d<sub>1</sub> and 5d<sub>2</sub> represent the two lowest 5d states and are both degenerate. c) Decay curves of the 0.5 at.% sample for  $Ce^{3+}$  emission when monitoring different wavelengths of the transitions from 5d<sub>1</sub>. d) Plot of lifetime against analyzing wavelength for the longer lifetime, 78.5–84  $\mu$ s ( $A = 0.85$ – $0.88$ ) obtained from biexponential fits (circles, using Equation (6)) and the monoexponential fits (triangles, using Equation (3a)).

due to faster migration and transfer to killer traps. In the present case, the nonradiative lifetime at different wavelengths is not known and it may vary also with wavelength. The general trend of measured lifetime (Figure 5d) is an increase with increasing wavelength, instead of the expected constant response.

#### 2.4.1. Conclusion

Although the lifetime of luminescence from one state under a constant environment in a crystal should be independent of emission wavelength, even for the same transition, the measured lifetime does vary experimentally with the monitoring wavelength due to numerous factors. To answer the question at the start of this section, normally the lifetime at the emission maximum is stated, but one must be aware of detector saturation effects.

It is therefore important to report the monitoring wavelength, in addition to the excitation wavelength, and monitoring time duration, when reporting lifetime data.

### 2.5. Average Lifetimes

#### 2.5.1. Multiexponential Decays

In cases of non-monoexponentiality of luminescence decay, as detected by inspection of the linearized plot (cf. Equation (3b,c)),

or simply pointed to by an unsatisfying value of  $R_{adj}^2$ , some authors apply a multiexponential model and then calculate average lifetimes. However, there are several definitions of the average lifetime.<sup>[22]</sup> We illustrate these parameters by using the emission decay results of YAG doped with 5 at.%  $Ce^{3+}$ , with the dataset normalized [0,1]. The higher concentration of  $Ce^{3+}$ , compared with that in Section 2.4, leads to a shorter lifetime ( $\approx 48$  ns using Equation (3a),  $R_{adj}^2 = 0.9905$ ), due to concentration quenching. Moreover, the decay deviates more from monoexponentiality.

First, for excited state donors surrounded by static acceptors (defects), acting as nonradiative recombination centers, when the emission decay is non-monoexponential due to a complex non-radiative process, the average lifetime  $\tau_1$  is:

$$\langle \tau_1 \rangle = \int_0^\infty I(t) dt / I(0) \quad (7)$$

Second, if the emission is non-monoexponential because there is a distribution of radiative rates, the average lifetime  $\langle \tau_2 \rangle$  is:

$$\langle \tau_2 \rangle = \int_0^\infty t I(t) dt / \int_0^\infty I(t) dt \quad (8)$$

In using these equations, since the integration limit is from zero time, we have normalized the dataset [0,1]. For the total

**Table 2.** Comparison of average lifetimes for YAG:Ce<sup>3+</sup> 5 at.% at RT:  $\lambda_{\text{exc}} = 460$  nm,  $\lambda_{\text{em}} = 530$  nm, measurement range 0–800 ns. Figures in brackets indicate the maximum deviation.

Item	Symbol	Equation	Magnitude [ns]
Average lifetime	$\langle \tau_1 \rangle$	(7)	46.8
Average lifetime	$\langle \tau_2 \rangle$	(8)	78.8
Intensity-weighted lifetime	$\langle \tau \rangle_{\text{iw}}$	(9)	59.2(8)
Amplitude-weighted lifetime	$\langle \tau \rangle_{\text{aw}}$	(10)	44.7(4)

decay in the region 0–800 ns, the calculated lifetimes  $\langle \tau_1 \rangle$  and  $\langle \tau_2 \rangle$  are 46.8 and 78.8 ns, respectively (Table 2).

Third, if the emission decay is not monoexponential but can be fitted by a biexponential or multiexponential function, representing two or more types of emitters, the average lifetime can be expressed as the intensity-weighted lifetime,  $\langle \tau \rangle_{\text{iw}}$  or amplitude-weighted lifetime  $\langle \tau \rangle_{\text{aw}}$ . Taking the biexponential case in Equation (6):

$$\langle \tau \rangle_{\text{iw}} = (A\tau_1^2 + B\tau_2^2)/(A\tau_1 + B\tau_2) \quad (9)$$

$$\langle \tau \rangle_{\text{aw}} = (A\tau_1 + B\tau_2)/(A + B) \quad (10)$$

The biexponential fit (Equation (6)) of the entire curve gives  $\tau_1 = 13.46(9)$  ns ( $A = 0.388(2)$ ) and  $\tau_2 = 65.5(1)$  ns ( $B = 0.582(2)$ ) ( $R_{\text{adj}}^2 = 0.9994$ ), so that  $\langle \tau \rangle_{\text{iw}} = 59.3$  ns, and  $\langle \tau \rangle_{\text{aw}} = 44.4$  ns. The reader is referred to the discussion of uses of  $\langle \tau \rangle_{\text{iw}}$  and  $\langle \tau \rangle_{\text{aw}}$  elsewhere.<sup>[11a,23]</sup> The intensity-weighted lifetime usually refers to the average lifetime of a collection of different excited-state populations. The amplitude-weighted lifetime can be used to estimate energy transfer efficiency.

**Conclusion:** Choose the relevant average lifetime which is appropriate for your application and define it. There are significant differences in the magnitudes of these parameters.

### 2.5.2. Stretched Exponential Decays

Many relaxation phenomena in physics are complex and cannot be modeled by (multi)exponential models but, rather, they obey a stretched exponential (or Kohlrausch) function:<sup>[24]</sup>

$$I(t) = \exp^{-(t/\tau_{\text{st}})^\beta} \quad \text{with} \quad 0 < \beta \leq 1 \quad (11)$$

where  $\tau_{\text{st}}$  (unit: s) provides an average over the fast early rates and slow long-lived rates. The parameter  $\beta$  represents the degree to which the measured decay differs from a purely exponential decay ( $\beta = 1$ ).<sup>[24]</sup>

This function is flexible and is applied empirically, even if a corresponding supporting model is not available.<sup>[25]</sup> This happens for instance for the luminescence of semi-conductor phosphors featuring a random distribution of trap states, such as CdS quantum dots for which  $\beta = 0.5$ .<sup>[26]</sup> This type of function has been applied recently in the analysis of the luminescence decay of Er<sup>III</sup> in a pseudo core-shell structure in which Er<sup>3+</sup> coordinated to a fluorinated organic ligand fitted with a triazole linker at its outskirt bearing aromatic groups. The Er<sub>x</sub>Y<sub>1-x</sub>L<sub>3</sub> systems studied have non-exponential luminescence decay that were

modeled with Equation (11); the extracted  $\beta$  values vary between 0.5 and 0.73 depending upon the concentration of Er<sup>3+</sup>.<sup>[27]</sup>

### 2.6. Why Do Biexponential Functions Often Adequately Fit Persistent Luminescence Decays?

Persistent luminescence is distinct from phosphorescence and often involves thermally activated emission from a chromophore by transfer of the excitation energy from trap (storage) states (Figure 6a,b). Figure 6c shows the RT persistent luminescence spectrum of hexagonal CsCdCl<sub>3</sub> doped with 1 at.% Mn<sup>2+</sup>, after charging with UV-excitation at 300 nm for 10 min. The emission, upon removal of the excitation source, is due to the <sup>4</sup>T<sub>1</sub> → <sup>6</sup>A<sub>1</sub> transition of Mn<sup>2+</sup>, which is thermally populated from the traps. The normalized persistent luminescence decay, Figure 6d can also be fitted by other equations but here we focus upon Equation (6), as subsequently described.

We have equated the normalized counts of emission to the population of the trap states that lead to emission from Mn<sup>2+</sup>. The logic is that the trap → Mn<sup>2+</sup> energy transfer rate is dependent upon trap depth (and hence temperature) if it is an activation process, and the lifetime of Mn<sup>2+</sup> at the ms scale is negligible compared with the longer timescale of persistent luminescence. The trap levels are not discrete but possess inhomogeneous broadening.

Then, we fitted different temporal regimes, for example: from monitoring time 0–10 s; from 0 to 20 s... etc. by monoexponential fits (Equation (3a)) and obtained a lifetime  $\tau$  in each case. The adjusted coefficients of determination,  $R_{\text{adj}}^2$ , were between 0.997 and 0.993.

These lifetime values are plotted against the end time of monitoring in Figure 6e. The lifetimes become longer for longer monitoring times and the graph can be fitted by a monoexponential function, as shown in Figure 6e. We interpret these results to show that the lifetime becomes longer when populating the excited state of Mn<sup>2+</sup> since the activation energy required to empty a deeper trap becomes greater. The shallower traps empty first. The rate of trap emptying has an exponential dependence with activation energy and is faster for more shallow traps.

The fitted red curve in Figure 6d is the biexponential fit (Equation (6)) to the entire persistent luminescence decay,  $R_{\text{adj}}^2 = 0.9993$ , with one long lifetime (46.6(0) s) and one shorter lifetime (7.7(0) s). The monoexponential fit in the inset of the same figure shows the lifetime of 38.2(0) s with  $R_{\text{adj}}^2 = 0.9929$ . From Figure 6e, since the lifetime increases with time, it is evident that the persistent luminescence decay will be fitted better by using two lifetimes than using just one. Hence, this is the simple reason that biexponential fitting is superior to monoexponential fitting of persistent luminescence. In fact, including another exponential term in the fit (triexponential) more closely fits to the decay, with  $\tau$  values of 72.7, 31.0 and 3.7 s ( $R_{\text{adj}}^2 = 0.9999$ ).

#### 2.6.1. Conclusion

The lifetime of persistent luminescence changes according to the measurement period because it depends on whether shallow or



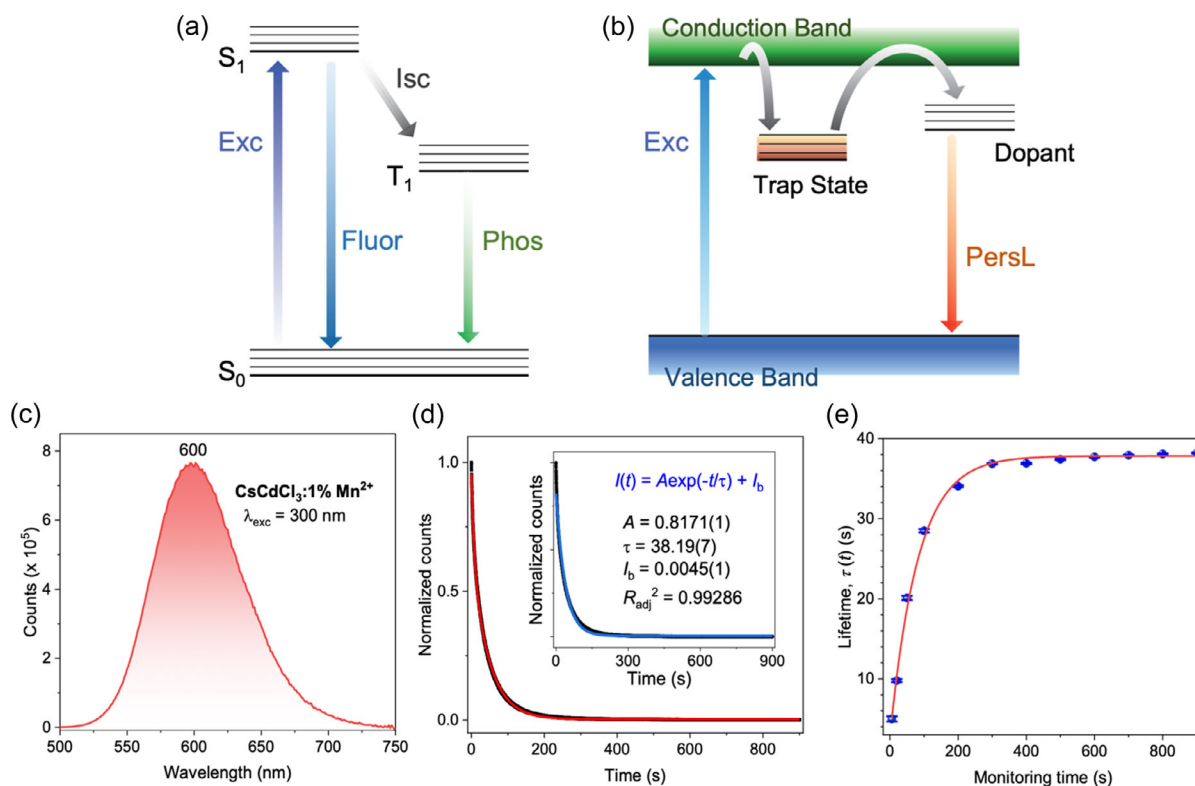


**Figure 6.** a) Distinction between phosphorescence (Phos) (a) and persistent luminescence (PersL), b) since both can have long lifetimes. In the first case, the compound is excited (Exc) to a singlet state which can fluoresce (Fluor) and/or undergo intersystem crossing (Isc) to a triplet state which then may emit radiation by phosphorescence (Phos). By contrast, one scenario of PersL involves excitation into the conduction band, or a lower state if available, and then storage (charging) in a trap state. When thermally activated, excitation transfer to the dopant ion can occur, followed by emission, PersL. c) Persistent luminescence spectrum of hexagonal  $\text{CsCdCl}_3$  doped with 1 at.%  $\text{Mn}^{2+}$  after charging for 10 min, using 300 nm UV radiation. d) Normalized persistent luminescence decay (black). The red line shows a fit by Equation (6). Fitted parameters:  $A = 0.299(1)$ ,  $B = 0.6653(0)$ ,  $I_b = 0.0027(0)$ ,  $\tau_1 = 7.6(0)$  s,  $\tau_2 = 46.6(0)$  s. The inset shows the corresponding fit by the monoexponential function Equation (3a) in blue. Fitted parameters:  $I(0) = 0.8171(1)$ ,  $I_b = 0.0045(1)$ ,  $\tau = 38.2(0)$  s. e) Plot of the lifetimes obtained by the monoexponential fit  $\tau(t) = \tau_\infty + \tau(0)\exp(-\tau/B)$  for selected monitoring periods, from 0 to  $t$ s, from the start of persistent luminescence decay in (c). Fitted parameters  $B = 81.8(4.8)$  s,  $\tau_\infty = 37.8(1)$  s, and  $\tau(0) = -35(1)$  s.

slightly deeper traps are being emptied. It becomes longer at longer times. Biexponential fits are better than monoexponential fits because they take this into account by employing short and long lifetimes as an average of the increasing lifetime. The derived parameters, however, have a restricted meaning.

## 2.7. What Is the Precision of Measuring a ns Lifetime Using a ns Pulse?

Many scientists in biosciences work with organic dyes that have noticeably short lifetimes, i.e., in the ns range.<sup>[28]</sup> Their equipment is, however, often limited to lasers emitting light pulses in the ns second range too, and photomultiplier detectors.<sup>[29]</sup> Therefore, the question arises as to whether measurements of ns lifetimes with such light sources are meaningful. We illustrate the case by choosing the popular endoplasmic reticulum (ER) tracer dye ER-Tracker-Green, **Figure 7a**; it is a derivative of BODIPY coupled with the oral hypoglycemic drug Glibenclamide, which has a highly selective binding to the endoplasmic reticulum, and it is non-toxic to cells at low concentrations. The dye is

cell-permeant and a highly selective stain for the endoplasmic reticulum in live cell imaging. **Figure 7b** shows the RT excitation and emission spectra of the dye at 10  $\mu\text{M}$  concentration in water. The emission maximum is at 511 nm and the Stokes shift is small: 10 nm.

In this case, the excitation pulse decay and the sample decay overlap to some extent. Lakowicz<sup>[8e,f]</sup> advises to use a zero-decay time scattering sample to measure the prompt. However, because of the small Stokes shift of the sample, the measured wavelengths are different for the sample and the prompt, and this can lead to color effects in the photodetector. Instead of using a metal plate for the prompt, one can use a standard with a very short lifetime which emits at the same wavelength as the sample. It is then assumed that the measured response is the instrument response. Another approach,<sup>[8e,f]</sup> is to employ a standard with known lifetime which emits at the same wavelength as the sample. A list of such standards with tabulated monoexponential lifetimes is given in the book of Lakowicz.<sup>[8e,f]</sup>

In the present case, subtraction of the normalized prompt and the sample decay over the range 0–50 ns leads to a rise and decay

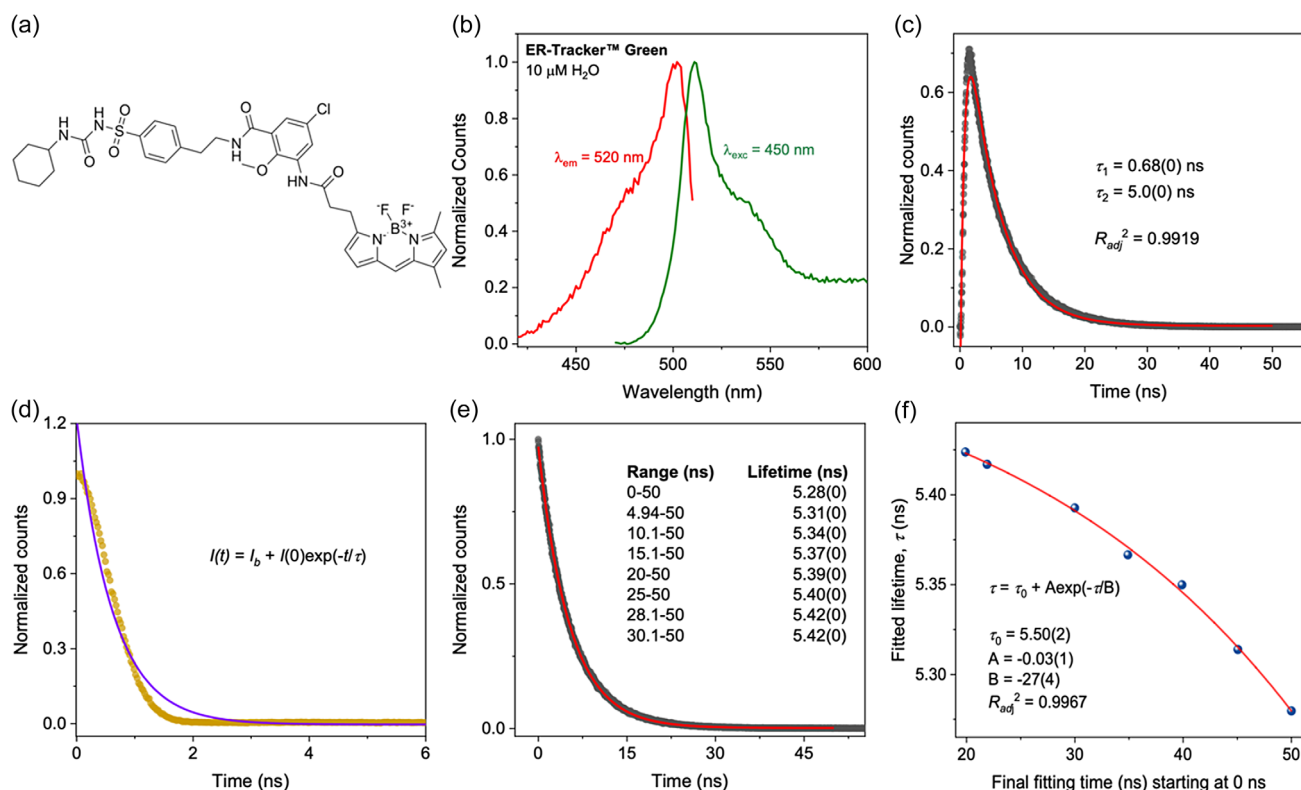


**Figure 7.** a) Formula of ER-Tracker-Green dye. b) Emission spectrum of the dye at 10  $\mu\text{M}$  concentration in water, using 450 nm excitation. c) Subtraction of the prompt from the dye decay, with both [0,1] normalized. d) Monoexponential fit (blue) of prompt (orange). e) Monoexponential fits of dye decay for different ranges. f) Fitted monoexponential lifetimes from e) plotted against length of measurement range.  $\tau_0$ ,  $A$  and  $B$  are fitting parameters.

of emission, Figure 7c, because the prompt decay is far from monoexponential (Figure 7d). However, the prompt decay is short  $\tau \approx 0.6 \text{ ns}$  compared to the sample lifetime  $\approx 5 \text{ ns}$ , the prompt contribution to the decay has completely vanished after  $\approx 10 \text{ ns}$ . Hence, we have fitted the lifetime using different time delays starting from the first one at 0 ns up to the one starting at 30.1 ns, Figure 7e. The fitted lifetime becomes longer when moving away from the start at 0 ns, and the values can be fitted by a monoexponential function, Figure 7f. There are several explanations for this. First, and most likely in the present case, the shorter ranges contain contributions from the fast prompt, leading to shorter lifetimes. Another explanation is that the local environment of dye molecules differs slightly, leading to a dispersion of lifetimes. Since some molecules have faster decay their contribution at longer times is less, so the measured lifetime increases.

The experimental process was repeated five times with reinitialization of the software and detector every time. The resulting error between the five measurements was found to be below 1%.

### 2.7.1. Conclusion

One must use care when measuring ns lifetimes using a ns pulsed laser, by examining the pulse shape and duration. Subtraction of the prompt may not be feasible. Several methods for the lifetime measurement in this timescale have been given by Lakowicz.<sup>[8e,f]</sup>

## 2.8. Summary and what Other Parameters Are Critical when Measuring Lifetimes?

- 1) Record the lifetime decay over an appropriate timescale, such as between 5 and 10 times the estimated lifetime value. Check the derived parameter values (Section 2.3).
- 2) Check the decay for short and long times after the laser pulse. At short times, traps or defect sites in inorganic phosphors may produce a fast component, or a slow rise; the long tail of the decay represents random noise and/or migration between activator ions.
- 3) The value of  $I_b$  is critical and incorrect values lead to incorrect lifetimes (Section 2.2; above, Table 1; Figure 3e). In some cases,  $I_b$  may be taken as the zero intensity/counts before the laser pulse. Some instruments do not permit observation of this before the laser pulse. It is usually kept as an adjustable parameter.
- 4) Trimming the first part of the lifetime curve (Figure S8b, Supporting Information), or recording for longer timescales (Figure 4b; Figure 7f), usually leads to a different lifetime value.
- 5) Reducing the number of datapoints fitted, whilst keeping the same calculation range generally gives similar fitted lifetimes, with increasing statistical error for fewer datapoints (Section 2.8.3).
- 6) Widening the entrance slit (Section 2.8.1) or saturating the detector (Section 2.8.2) can drastically change the recorded lifetime value. Saturation effects can be checked by using a neutral density filter and re-recording the lifetime decay. Reduce the slit width of the emission monochromator until a constant lifetime is obtained.

### 2.8.1. Conclusion

In view of the many factors involved, all experimental conditions used to measure the decay and all the details regarding the fitting procedure should be given when reporting luminescence lifetimes. Moreover, and importantly, lifetime values should not be reported at too high precision. Real experimental errors, and not only reproducibility or statistical error from the fitting procedure, should be given.

## 3. Take Home Messages

The lifetime measurement is a good yardstick of the sample purity. A perfectly exponential decay represents an uncontaminated sample. All chromophores have the same environment and hence the same lifetime, even for transitions to different terminal states from the same initial state. Normally, the determined lifetime will differ if different ranges or different emission wavelengths are employed for its measurement. Different fitting methods give different results.

We estimate that the usual precision of lifetime determination is between 2% and 3%, although as demonstrated earlier, results may differ by as much as nearly 10% depending on experimental factors and models used for fitting the decays. When reporting an emission lifetime, besides the sample details and temperature, include the excitation source and wavelength, the emission wavelength, the measurement range, and the fitting procedure. The experiment should be repeated at least three times on each of at least two different samples of the materials investigated to enable the experimental error to be calculated. This is seldom, if ever, done. Do not overestimate the precision.

## Supporting Information

Supporting Information is available from the Wiley Online Library or from the author.

## Acknowledgements

K.-L.W. thanks the financial assistance from the Hong Kong Research Grants Council No. 12300021, NSFC/RGC Joint Research Scheme (N\_PolyU209/21). We thank Mr. Daiwen Xiao for providing the dataset in Section 2.6.

## Conflict of Interest

The authors declare no conflict of interest.

## Keywords

experimental parameters, fitting procedure, kinetic model, lifetime, luminescence

Received: May 17, 2024

Revised: June 24, 2024

Published online: July 15, 2024

- [1] J. R. Lakowicz, *Principles of Fluorescence Spectroscopy*, Springer US, Boston, MA **2006**, pp. 1–26, Ch. 1.
- [2] a) K. Ishii, T. Tahara, *J. Phys. Chem. B* **2013**, *117*, 11423; b) J. Alcala, E. Gratton, F. Prendergast, *Biophys. J.* **1987**, *51*, 587.
- [3] V. C. Ferricola, L. Rosso, R. Galleano, T. Sun, Z. Y. Zhang, K. T. V. Grattan, *Rev. Sci. Instrum.* **2000**, *71*, 2938.
- [4] M. Tan, F. Li, N. Cao, H. Li, X. Wang, C. Zhang, D. Jaque, G. Chen, *Small* **2020**, *16*, 2004118.
- [5] A. L. James, C. Pei-Hua, S. Klaus, *J. Biomed. Opt.* **2015**, *20*, 096002.
- [6] a) M. Y. Berezin, S. Achilefu, *Chem. Rev.* **2010**, *110*, 2641; b) Z. Zang, D. Xiao, Q. Wang, Z. Li, W. Xie, Y. Chen, D. D. Li, *Sensors* **2022**, *22*, 3758; c) W. Becker, *J. Microsc.* **2012**, *247*, 119.
- [7] T. Moriya, *Bull. Chem. Soc. Jpn.* **1984**, *57*, 1723.
- [8] a) J. Demas, *Excited State Lifetime Measurements*, Academic Press Inc, New York, NY **1983**; b) S. Isbaner, N. Karedla, D. Ruhlandt, S. C. Stein, A. Chizhik, I. Gregor, J. Enderlein, *Opt. Express* **2016**, *24*, 9429; c) B. B. Collier, M. J. McShane, *J. Lumin.* **2013**, *144*, 180; d) G. E. Khalil, K. Lau, G. D. Phelan, B. Carlson, M. Gouterman, J. B. Callis, L. R. Dalton, *Rev. Sci. Instrum.* **2004**, *75*, 192; e) J. R. Lakowicz, *Principles of Fluorescence Spectroscopy*, Springer US, Boston, MA **2006**, pp. 97–155, Ch. 4; f) J. R. Lakowicz, *Principles of Fluorescence Spectroscopy*, Springer US, Boston, MA **2006**, pp. 157–204, Ch. 5; g) U. Noomnarm, R. M. Clegg, *Photosynth. Res.* **2009**, *101*, 181.
- [9] Edinburgh Instruments, Technical Note: Measurement of Photoluminescence lifetimes in the  $\mu$ s Range, [https://www.edinst.com/wp-content/uploads/2018/06/TN\\_48-Measurement-of-Photoluminescence.pdf](https://www.edinst.com/wp-content/uploads/2018/06/TN_48-Measurement-of-Photoluminescence.pdf) (accessed: April 2024).
- [10] a) W. Becker, *Advanced Time-Correlated Single Photon Counting Techniques*, Springer-Verlag, Germany **2006**; b) W. Hwang, D. Kim, S. Lee, Y. J. Won, S. Moon, D. Y. Kim, *Opt. Commun.* **2019**, *443*, 136.
- [11] a) Y. Li, S. Natakorn, Y. Chen, M. Safar, M. Cunningham, J. Tian, D. D.-U. Li, *Front. Phys.* **2020**, *8*, 576862; Y. Li, S. Natakorn, Y. Chen, M. Safar, M. Cunningham, J. Tian, D. D.-U. Li, *Erratum in: Front. Phys.* **2021**, *8*, 637953; b) P. J. Butterworth, F. J. Warren, T. Grassby, H. Patel, P. R. Ellis, *Carbohydr. Polym.* **2012**, *87*, 2189; c) J. R. Ward, L. J. Decker, *Ind. Eng. Chem. Prod. Res. Dev.* **1982**, *21*, 460; d) J. R. Bacon, J. Demas, *Anal. Chem.* **1983**, *55*, 653.
- [12] a) L. N. Puntus, K. J. Schenk, J. C. G. Bünzli, *Eur. J. Inorg. Chem.* **2005**, *2005*, 4737; b) G. Brito-Santos, B. Gil-Hernández, I. R. Martín, R. Guerrero-Lemus, J. Sanchiz, *RSC Adv.* **2020**, *10*, 27815.
- [13] S. Meshkova, Z. Topilova, D. Bolshoy, S. Beltyukova, M. Tsvirko, V. Y. Venchikov, *Acta Phys. Pol., A* **1999**, *95*, 983.
- [14] M. Kleinerman, S.-I. Choi, *J. Chem. Phys.* **1968**, *49*, 3901.
- [15] A.-S. Chauvin, S. Comby, B. Song, C. D. B. Vandevyver, J.-C. G. Bünzli, *Chem. Eur. J.* **2008**, *14*, 1726.
- [16] H. Feng, D. Ding, H. Li, S. Lu, S. Pan, X. Chen, G. Ren, *J. Alloys Compd.* **2011**, *509*, 3855.
- [17] T. Yanagida, T. Kato, D. Nakauchi, N. Kawaguchi, *Sens. Mater.* **2024**, *36*, 443.
- [18] L. Canty, S. Hariharan, Q. Liu, S. A. Haney, D. W. Andrews, *PLoS One* **2018**, *13*, e0208075.
- [19] T. Kellerer, J. Janusch, C. Freymüller, A. Rühm, R. Sroka, T. Hellerer, *Int. J. Mol. Sci.* **2022**, *23*, 15885.
- [20] F. Witte, P. Rietsch, N. Nirmalanathan-Budau, F. Weigert, J. P. Götze, U. Resch-Genger, S. Eigler, B. Paulus, *Phys. Chem. Chem. Phys.* **2021**, *23*, 17521.
- [21] a) H. Dornauf, J. Heber, *J. Lumin.* **1980**, *22*, 1; b) R. J. Bateman, R. R. Chance, J. F. Hornig, *Chem. Phys.* **1974**, *4*, 402.

- [22] G. Zatoryb, M. Klak, *J. Phys.: Condens. Matter* **2020**, 32, 415902.
- [23] A. Sillen, Y. Engelborghs, *Photochem. Photobiol.* **1998**, 67, 475.
- [24] H. Wen, P. A. Tanner, *Opt. Mater.* **2011**, 33, 1602.
- [25] M. N. Berberan-Santos, E. N. Bodunov, B. Valeur, *Chem. Phys.* **2005**, 315, 171.
- [26] J. E. Martin, L. E. Shea-Rohwer, *J. Lumin.* **2006**, 121, 573.
- [27] Y. Peng, J. X. Hu, H. Lu, R. M. Wilson, M. Motevalli, I. Hernández, W. P. Gillin, P. B. Wyatt, H. Q. Ye, *RSC Adv.* **2017**, 7, 128.
- [28] A. S. Kristoffersen, S. R. Erga, B. Hamre, Ø. Frette, *J. Fluoresc.* **2018**, 28, 1065.
- [29] D. M. Rayner, A. E. McKinnon, A. G. Szabo, *Rev. Sci. Instrum.* **1977**, 48, 1050.